An Improved Transmission-Line Model of Grounding System

Yaqing Liu, Mihael Zitnik, and Rajeev Thottappillil

***Abstract*—This paper presents a time-domain transmission line model of grounding system, which includes the mutual electromagnetic coupling between the parts of the grounding structure and the influence of air-earth interface. The model can be used to simulate the transient behavior of the grounding system under lightning strike. The simulation results are in good agreement with that of the model based on the solution of full Maxwell's equations [1], [2] and also with the measurements reported in [1]. The influence of different parameters, such as the soil relative permittivity ε_r, the soil resistivity ρ, and the conductivity and diameter of the conductor, on the transient voltage distribution of the grounding system is investigated. It shows that, among the parameters investigated here, the soil resistivity is the most important parameter that affects the transient response of bare buried conductors. The soil permittivity has very little influence on the transient response of the grounding system when the grounding system is buried in the soil with low resistivity, but have moderate influence in the soil with extremely high resistivity. The conductivity of the conductor and skin effect have practically no influence on the peak transient voltage of the grounding system. Increase in conductor diameter tends to decrease the peak transient voltage. The model presented in this paper is simple, but sufficiently accurate and can be used easily in engineering practice. Since the model is in the time domain, it could be easily coupled to the other time-domain models of nonlinear surge-protection components.**

***Index Terms*—Grounding system, transmission line model.**

I. Introduction

DIFFERENT grounding systems, such as buried vertical and horizontal electrodes and large grounding grids, are often part of the lightning-protection system in industrial and power plants. Large impulse currents during a lightning strike could flow in the grounding system and induce large transient voltage before it is dissipated into the soil. These current surges and induced voltages could couple to equipments which are connected to the grounding system, and cause operation error, malfunction, or even destruction of important electronic equipment, especially for modern electronic circuits, which generally have low-signal levels and are sensitive to various kinds of electromagnetic disturbance. Consequently, electromagnetic compatibility (EMC) studies require the knowledge of the spatial and temporal distribution of voltages along the grounding system in the case of lightning.

A number of analytical models aimed for transient analysis of grounding system have been published. The analysis in [3] and [4] are based on the empirical approach, and the lumped circuit theory, respectively, with too many approximations. The transmission-line theory is used in [5], [6], but this model neglects the mutual electromagnetic coupling between the parts of the grounding structure, which introduce errors as shown in [7].

The electromagnetic-field model [1], [2], [8] is considered to be the most accurate because it applies the full Maxwell's equations with minimum possible approximations and hence it is used as a reference case to compare the results of the model presented here. In [1], the grounding grid is represented as thin cylindrical metallic conductors with finite conductivity. The soil is modeled as linear and homogeneous half-space characterized by conductivity, permittivity, and permeability constants. The influence of the air-earth interface is taken into account approximately by a modified image theory. However, this model describes and solves the problem in the frequency domain, so, it is not easy to combine the grounding system with other nonlinear surge-protection components which are modeled in the time domain. Moreover, the electromagnetic field model is computationally too complex to be applied in engineering practice. We present, in this paper, an improved time-domain transmission-line model which is easily solved in the popular software, Alternate Transient Program of the Electromagnetic Transient Program (ATP-EMTP) [10]. The parameters for the transmission line is calculated using Ace [9]. However, any other suitable electromagnetic fields software could be used in place of Ace. The model includes the effect of mutual coupling between the conductors and the effect of air-earth interface.

This paper is organized as follows. First, the methodology of the model is briefly described. In the second part, this model is applied to a buried horizontal conductor and the 1×1, 2×2 grounding grids. The results are compared with [1], [2]. The third part investigates the influence of different parameters of the soil and conductor system on the transient behavior of the grounding system, and gives an explanation from the point of the electric-circuit theory, which makes the complex transient phenomena of the grounding system easily understandable.

II. Description of the Methodology

A. Basic Assumptions

The grounding systems are structured with good conductors. Every conductor is assumed to be part of a lossy transmission line. It is also assumed that the radii of the conductors are uniform at any point along the conductors and much smaller than the wavelength and the wires' length. The conductor is characterized by its electric properties and dimensions. The soil is modeled as linear and homogeneous half-space characterized by resistivity, relative permittivity, and permeability constants.

Manuscript received October 18, 2000; revised January 15, 2001.

The authors are with the Division for Electricity and Lightning Research, Ångström Laboratory, Uppsala University, Sweden.

Publisher Item Identifier S 0018-9375(01)07136-8.

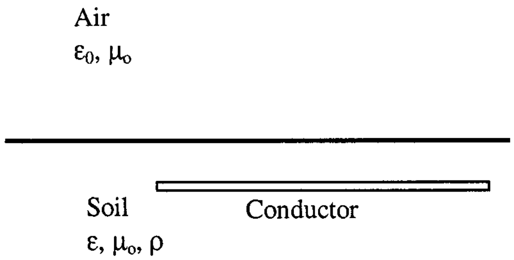

Fig. 1. Illustration of the physical situation.

Consequently, the soil is a lossy medium. The current is partly flowing along the conductors, and partly is dissipated into the soil. Here, the ionization of the soil is not considered. The skin effect of the conductor is neglected (in the third part, we will show the reason). The electromagnetic field surrounding the conductors is the quasitransverse electromagnetic (quasi-TEM) field, neglecting the fringing influence at the end points.

Practical grounding systems have some conducting structure above the ground also (e.g., air-termination, and down conductors of the lightning protection system), in addition to the buried conductors. Any magnetic coupling between the overground system and underground system are not considered. Besides, the vertical conductor that connects the buried grounding system with the overground system, are also not considered. The surge current is assumed to be injected directly to the grounding grid.

B. Per-Unit Length Parameters of the Conductor

Since the conductor is assumed to be part of a transmission line, calculating all kinds of per-unit length parameters, such as resistance, self or mutual inductance, capacitance and conductance, is the first step. Per-unit length resistance can be easily calculated by the analytical equation. However, analytical solutions for self and mutual capacitance and conductance are complex in the presence of air-soil interface [11], especially if the grounding system buried in the soil is electrically close to the air-soil interface (see Fig. 1). The inductance is not influenced by the air-soil interface because the soil permeability μ is the same as that of the air. However, the analytical solutions for the inductance are also complex when the grounding system is a large grounding grid.

In this paper, the electromagnetic-field analysis program Ace is applied to calculate these per-unit length parameters except resistance, according to the geometries of the grounding system. Consequently, the influence of the air-soil interface can be included.

In Ace, the simulation of the problem is performed by solving the Maxwell differential equations according to the finite-element method or method of moment. In this paper, finite-element method is applied. In fact, any other suitable electromagnetic software can be used to find the per-unit length parameters of transmission lines according to the following equations. In (2)–(7), the reference boundary is chosen very far away from the conductor system, which simulates the fact that lightning-surge currents in grounding systems do not have a return conductor or the 'return conductor is at infinity'. Calculated parameters are insensitive to the chosen boundary.

1) Per-unit length resistance

$$r = \frac{\rho_c}{s_0} \tag{1}$$

where

- r per-unit length resistance of the conductor;
- ρ_c resistivity of the conductor;
- s_0 cross section area of the conductor.

2) Per-unit length inductance

According to the equation of the energy stored in solenoidal magnetic field [12], $w_l = 1/2LI^2$, the per-unit length inductance could be calculated as follows:

$$l_{ii} = 2\frac{\int_s \left(\int_0^B H \cdot dB\right) ds}{I_i^2} \tag{2}$$

where

- l_{ii} self-partial inductance;
- I_i current flowing along with the ith conductor;
- $\int_s \left(\int_0^B H \cdot dB\right) ds$ magnetic-field energy caused by I_i;
- s cross-section area between the ith conductor and the reference boundary.

Additionally

$$l_{ij} = \frac{\int_s \left(\int_0^B H \cdot dB\right) ds - \frac{I_i^2 l_{ii} + I_j^2 l_{jj}}{2}}{I_i I_j} \tag{3}$$

where

- l_{ij} mutual-partial inductance;
- I_i,I_j currents flowing along with the ith and jth conductor;
- $\int_s \left(\int_0^B H \cdot dB\right) ds$ total magnetic-field energies caused by I_i and I_j;
- $I_i^2 l_{ii}/2$,$I_j^2 l_{jj}/2$ magnetic-field energies caused by self-partial inductances l_{ii} and l_{jj}, respectively.

3) Per-unit length capacitance

$$c_{ii} = \frac{\int_{s_i} D \cdot ds}{V_i} \tag{4}$$

where

- c_{ii} self-partial capacitance which is sum of all mutual capacitances and capacitance to the earth;
- V_i potential of the ith conductor with respect to the infinite earth, while the potentials on the other conductors are set to zero;
- $\int_{s_i} D \cdot ds$ charges deposited on the ith conductor per-unit length because of V_i;
- s_i integral surface around the conductor.

Additionally

$$c_{ij} = \frac{\int_{s_j} D \cdot ds}{V_i} \tag{5}$$

- c_{ij} mutual-partial capacitance;
- $\int_{s_j} D \cdot ds$ charge deposited on the jth conductor per-unit length because of V_i;
- s_j integral surface around the conductor.

4) Per-unit length conductance

$$g_{ii} = \frac{\int_{s_i} j_n \cdot ds}{V_i} \tag{6}$$

where

- g_{ii} self-partial conductance which is sum of all mutual conductances and conductance to the earth;
- V_i potential of the ith conductor with respect to the infinite earth, while the potentials on the other conductors are set to zero;
- $\int_{s_i} \vec{j}_n \cdot d\vec{s}$ current which is perpendicular to the surface of the ith conductor and flowing to the earth per-unit length because of V_i;
- s_i integral surface around the conductor.

And

$$g_{ij} = \frac{\int_{s_j} j_n \cdot ds}{V_i} \tag{7}$$

- g_{ij} mutual-partial conductance;
- $\int_{s_j} \vec{j}_n \cdot d\vec{s}$ current which is perpendicular to the surface of the jth conductor and flowing to the earth per-unit length because of V_i;
- s_j integral surface around the conductor.

In order to see the influence of the air-soil interface, per-unit length parameters of a horizontal copper wire buried at 0.6-m depth in the soil are calculated. The computation results with and without the influence of the air-soil interface are compared. For this comparison, the following parameters are assumed. The radius of the wire is 25.45 mm and the length is 60 m. The resistivities of the copper and soil are 1.72×10^{-8} Ωm and 125 Ωm, respectively. The relative soil permittivity ε_r and permeability μ_r are 36 and 1.

The computation results with the influence of the air-soil interface for self-partial inductance, conductance, and capacitance are $l_{\text{withair}} = 1.085$ μH/m, $g_{\text{withair}} = 6.50 \times10^{-3}$ /Ωm, and c_{withair} =271 pF/m, respectively, while the results of neglecting the influence of the air-soil interface are l_{noair} =1.085 μH/m, $g_{\text{noair}} = 8.90\times10^{-3}$ /Ωm, c_{noair} =355 pF/m. There is no difference in the self-partial inductance, which is not surprising because the relative permeability of the soil and air are assumed to be unity. The self-partial conductance and capacitance with the assumption of uniform soil mediums (no air-soil interface) are higher by 37% and 31%, respectively, when compared with the case in which the air-soil interface is considered. It is clear that we cannot neglect the influence of the air-soil interface, which can not be considered in old transmission line model of the grounding system [7].

There are also techniques [15], [16] in which the influence of the air-earth interface is taken into account through the changes in propagation constant. However, it is easier for us to take into account the air-earth interface through the changes in per-unit length parameters since we are using the transmission-line model in time domain. Note that changed per-unit length parameters influence the propagation constant of the dissipative transmission line and hence both methods should give equivalent results.

It should be noticed that all the parameters are calculated by using the static-field analysis techniques, because the field structure for quasi-TEM mode of propagation is identical to a static (dc) field structure [13]. For a simple grounding system, such as a single buried horizontal conductor, there is no mutual per-unit parameters; for mesh grounding system, such as 1×1 and 2×2 grounding grids, mutual coupling should be considered between the parallel conductors, but not between the perpendicular conductors.

C. Transients of the Grounding System

The model of the grounding system in this paper is based on transmission-line theory, so, lumped circuit of the grounding system could be created if the transmission line is divided into many electrically small sections. Then, the transient behavior of the grounding system can be simulated by the ATP-EMTP, which is based on nodal equations. This program has been widely applied in power-system simulation, especially for transient phenomena.

In ATP-EMTP, every electrically small section of the transmission line is represented by lumped resistance R, inductance L, capacitance C and other coupling elements, if the per-unit length parameters of the conductors are known. The number of the sections required for a accurate simulation is dependent on the frequency components of the injection impulse.

III. Verification of the Model

A. Simulation of a Buried Horizontal Conductor

The radius of the horizontal copper conductor is 12 mm and the length is 15 m. It is buried at 0.6-m depth in the soil. The resistivities of the copper and soil are 1.72×10^{-8} Ωm and 70 Ωm, respectively. The relative soil permittivity ε_r and permeability μ_r are 15 and 1. The current impulse is injected in one end of the 15-m long horizontal wire. The wave shape of the current impulse is expressed by double-exponential form denoted by the equation$I(t) = I_0(\mathrm{e}^{-At} - \mathrm{e}^{-Bt})$.Here, I_0 is 36.5 A. A is 60 000 1/s, and B is 6 000 000 1/s. The time to the peak is 0.8 μs, which is defined as a time period from $I = 0$ to $I =$ maximum value (See Fig. 2), and the time to half-value is 12.5 μs, which is from $I = 0$ to $I = 50\%$ maximum value.

All these parameters of the system are the same as that of the reference [1], except the wave shape of the current impulse. In reference [1], the time to the peak of the current is about 0.8 μs, the same as in this paper, but the time to half value is not presented. However, the influence of the injection current is mainly dependent on the time to the peak [2]. Consequently, the current impulse, which is shown in Fig. 2, could be used to approximate the injection current of reference [1].

Fig. 3 shows the transient voltages to the remote ground at three points along the wire, which is simulated by using our improved time-domain transmission line model. These three points are located at $x = 0$ m, $x = 3.5$ m, and x =7 m, respectively, from the injection point at x =0 m. The amplitude of the transient voltage at the injection point of the wire is about 600 V at t =0.146 μ. For points x =3.5 m, and x =7 m, the maximum values of the transient voltages are 342 V at t =0.33 μs, and 228 V at t >0.7 μ, respectively. Comparing with the similar

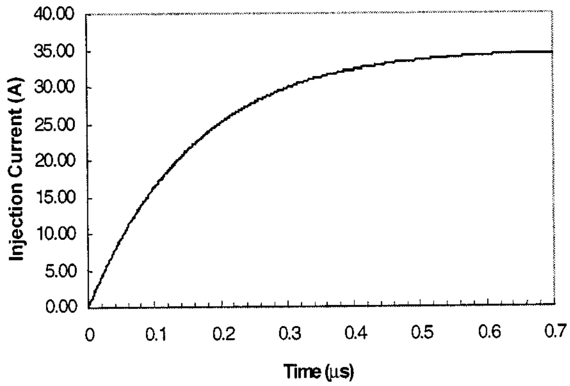

Fig. 2. The wave shape of the injection current.

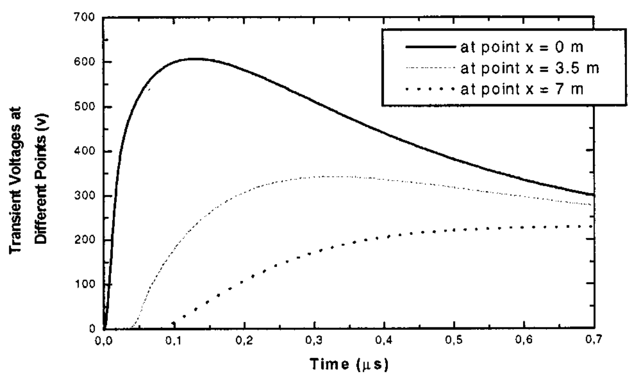

Fig. 3. The transient voltages to the remote ground at three points along the horizontal copper wire.

wire in [1], the difference of the maximum value of the transient voltages at points $x = 0$ m, x =3.5 m, and $x = 7$ m is about 5%–7%. The transient voltages reach their peaks before the applied current peak (See Figs. 2 and 3). This result is also seen in [1]. The reason for this time delay between the voltage peak and current peak could be that the inductance effect is dominant in this grounding system. All the simulation results in Fig. 3 and [1] are smaller than the measurement results, which is presented in reference [1], because of some remaining inductive voltage drop during the wave front along the resistive voltage divider which is used in measurement.

B. 1× 1 and 2×2 Grounding Grids

Two grounding grids are chosen for computations, 1×1 and 2×2 with dimensions 10 by 10 m [see Fig. 4(a)]. The diameter of the conductors is 14 mm. All grids are buried at 0.5 m depth in the homogenuous soil with $\rho = 1000\ \Omega$m and $\varepsilon_r = 9$. The rise time of the current impulse is defined as a time period which is from $I = 10\%$ to $I = 90\%$ maximum value. According to this definition, the rise time in reference [2] is about 0.3–0.4 μs. In our simulation, the double-exponential current impulse, $I(t) = 1\times(\mathrm{e}^{-27\,000t} - \mathrm{e}^{-5\,600\,000t})$ A, is chosen to approximate the injection currents used in [2]. The rise time is about 0.36 μs, the decay time, from $I = 0$ to $I = 50\%$ maximum value, is about 26.8 μs. The injection point is at point A, the corner of the grounding grid. All these parameters of the system are

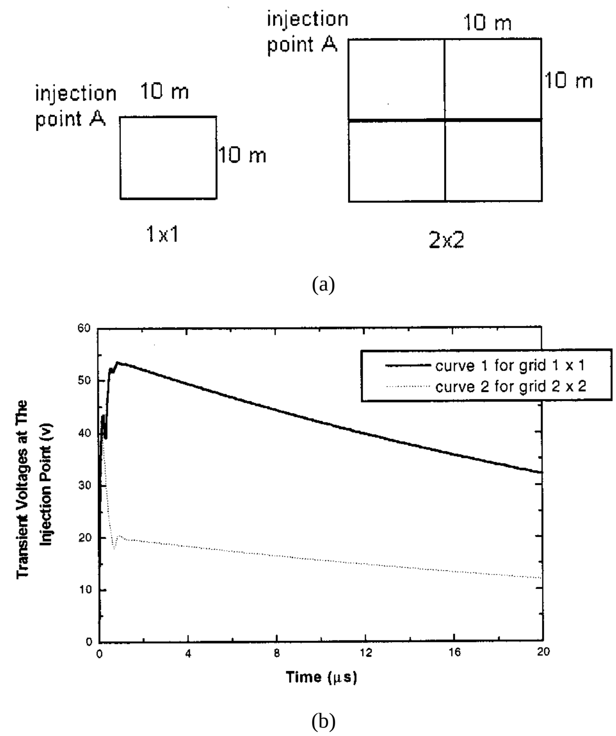

Fig. 4. (a) The dimensions of the two different grounding grids. (b) The transient voltages of grounding grids 1×1 and 2×2 at the injection point as response to the current impulse $I(t) = 1 \times (\mathrm{e}^{-27\,000t} - \mathrm{e}^{-5\,600\,000t})$ A.

selected, the same as that in [2], for comparing the result with that presented in [2].

Fig. 4(b) presents the simulation results of the maximal transient voltages at the injection point for two grids as response to the current impulse. The rise times of the transient voltages in our simulation are almost same as that in [2]. The maximum values are larger than the results of reference [2] by only 5%–8%. This difference may be caused by the following factors.

1) The injection current is not exactly same as that of reference [2]
2) Neglect of the fringing fields and its possible influence on the per-unit length parameters.
3) Neglect of the coupling between the perpendicular conductors
4) Neglect of the mutual conductive coupling between the conductors through the soil, because the per-unit length resistance between the conductors through the soil is about several ten kilohms, which is much larger than the per-unit length impedance of the mutual inductance between the conductors.

All these comparisons show that the good agreement is reached between our simulation results and that in [1], [2]. So, the model in this paper is not only suitable for the simple grounding conductor, but also can be used to simulate the transient behavior of the mesh grounding grid.

IV. The Influence of the Parameters

All the parameters of the grounding system, such as the soil relative permittivity ε_r, soil resistivity ρ, and the conductivity

(a) (b)

Fig. 5. Illustration of two 2×2 grounding grids with different conductor diameters.

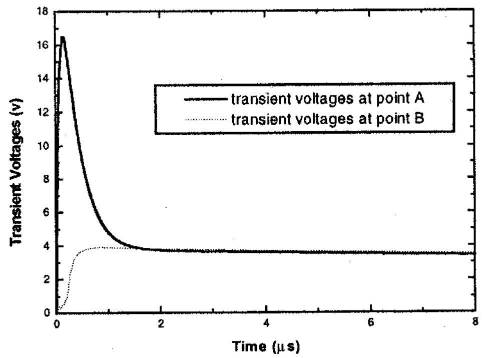

(a)

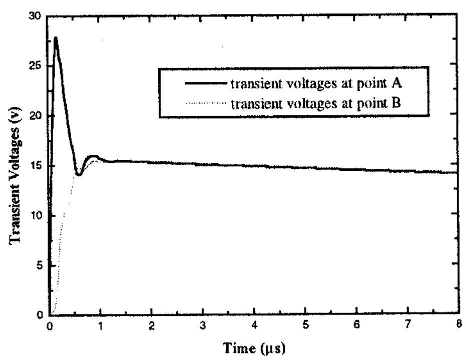

(b)

Fig. 6. The transient voltages of grid (a) at point A and B in the soils with different resistivities. (a) The soil resistivity is $\rho = 100\ \Omega$m. (b) The soil resistivity is $\rho = 400\ \Omega$m.

and diameter of the conductor, are related to the electric circuit elements through per-unit length parameters of the conductors in our improved time-domain transmission line model. So, the influence of these parameters can be explained from the point of the electric circuit theory.

In order to see the influence of the different parameters clearly, other two 2×2 grounding grids are used with dimensions 6 by 6 m (see Fig. 5). The diameter of the conductors are 14 mm for grid (a) and 40.4 mm for grid (b), respectively. The grids are buried at 0.6-m depth in different homogenous soils. The resistivity of the copper is $1.72\times10^{-8}\ \Omega$·m. The current impulse with the lightning-wave shape, $I(t) = 1 \times (\mathrm{e}^{-14\,300t} - \mathrm{e}^{-5\,400\,000t})$ A, is injected at the point A.

A. The Influence of the Soil Resistivity ρ

Fig. 6(a) and (b) shows the transient voltages to the remote ground at different points of grid (a) (see Fig. 5) buried in two types of soil with different resistivities, $\rho = 100\ \Omega$m, and $\rho = 400\ \Omega$m, but with same relative permittivity, $\varepsilon_r = 36$. Here, the mutual-capacitive coupling is not considered because its influence is negligible, which can be seen in the next section. The curves in Fig. 6(a) and (b) show that the transient voltage at injection point (point A) in the soil with high resistivity is larger than that in the soil with low resistivity. The peak transient voltage has increased by 70% when the soil resistivity is increased four times. Immediately, after the application of the transient, different points on the grounding system have different voltages (see points A and B in Fig. 6). Later, the voltages become equal. It is also found that the soil resistivity affects the equalized voltage on the surface of the grounding system greatly, not only the value, but also the time period which is needed for the system to reach this value. For the soil with ρ =400 Ω·m, the equalized voltage is 15.5 V, the time to reach this value is 1 μs. For the soil with ρ =100 Ω·m, the equalized voltage decreases to 3.8 V and the time to reach this value becomes 1.8 μs. Thus, a four-time increase in the soil resistivity produces a four-time increase in the equalized voltage.

According to the simulation, we found that, in the soil with high resistivity, the grounding system has large potential difference at different points, especially at the beginning of the current impulse. Moreover, even if it becomes an equal-potential system after few microseconds, the equalized voltage to the remote ground is much higher than that in the soil with low resistivity. These results can be explained as follows. In the soil with high resistivity, the conductance of the grounding conductors to the remote ground is much smaller than that in the soil with low resistivity, so, it is more difficult for the grounding system to dissipate the transient current into the soil and decrease the transient voltage of the grounding system to a lower value.

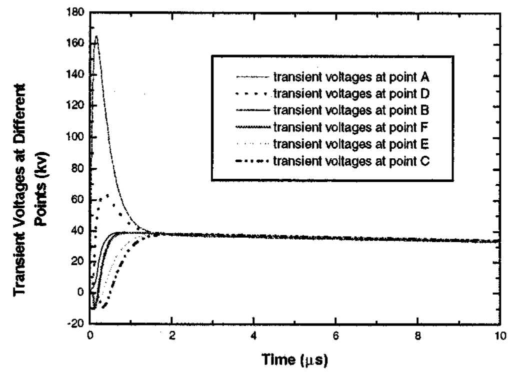

Fig. 7. The voltage distribution of the grounding grid (a) at six different points in the soil with $\rho = 100\ \Omega$m and $\varepsilon_r = 36$, as response to the lightning current impulse injected at point A, $I(t) = 10 \times (\mathrm{e}^{-14\,300t} - \mathrm{e}^{-5\,400\,000t})$ kA.

The problem of uneven voltage distribution is very important in the multipoint grounding system. Fig. 7 shows the transient voltage distribution of the grounding grid (a) (see Fig. 5) to the remote ground at six different points in the soil with ρ =100 Ω·m and $\varepsilon_r = 36$, as response to a lightning current impulse injected at point A, $I(t) = 10 \times (\mathrm{e}^{-14\,300t} - \mathrm{e}^{-5\,400\,000t})$ kA. The further is the point away from the point A, the lower is the voltage. For example, the maximum voltage difference between points D and C could be 70 kV at the beginning of the current impulse.

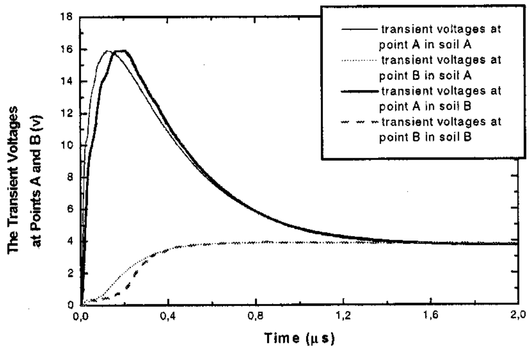

Fig. 8. The transient voltages of grid (a) at points A and B without considering the influence of mutual capacitances in two types of soil A ($\rho = 100\ \Omega$m, $\varepsilon_r = 9$) and B ($\rho = 100\ \Omega$m, $\varepsilon_r = 36$).

If a complex electrical system is connected to this grounding grid with the multipoint grounding methods, the subsystems are connected at different points on the grid. When the lightning current impulse happens to enter the grounding grid, different points have different potentials, as shown in Fig. 7. Then, unexpected current from the grounding grid might flow into the electric system and could cause serious EMC problems. If the resistivity of the soil is high, the problem becomes more serious because the voltage difference at different points is much larger at the beginning of the current impulse in the soil with high resistivity, as can be seen in Fig. 6(b).

B. The Influence of the Soil Permittivity ε_r

The influence of the soil relative permittivity ε_r is related to the capacitive coupling between the conductors of the grounding system because the soil is a dielectric medium. So, it is obvious that the influence of the soil permittivity is effective through the influence of the self and mutual capacitance of the grounding conductors on the transient behavior of the grounding system. The simulation shows that the results are different in the soil with low resistivity ($\rho = 100\ \Omega$ m), compared with that in the soil with extremely high resistivity ($\rho = 200\ \Omega$ m).

In order to investigate the influence of the permittivity ε_r in the soil with lower resistivity, two types of soil, A ($\varepsilon_r = 9$, $\rho = 100\ \Omega$m) and B ($\varepsilon_r = 36$, $\rho = 100\ \Omega$m), are chosen. Grid (a) in Fig. 5 is the grounding system. The current impulse is $I(t) = 1 \times (\mathrm{e}^{-14\,300t} - \mathrm{e}^{-5\,400\,000t})$ A.

Fig. 8 displays the influence of the self and mutual capacitance. Even though ε_r increases four times from soil A ($\varepsilon_r = 9$) to Soil B ($\varepsilon_r = 36$), and the capacitance increases four times too, the transient voltages to the remote ground at point A and B have no obvious difference. The simulation which does not include the influence of the mutual capacitance shows the same results, except that the peak value of the transient voltages at point A is 3% larger in soil B compared with that in soil A. That is why in the previous subsection A, we neglected the influence of the mutual capacitance.

When the grounding grid (a) in Fig. 5 is buried in the soil with very high resistivity, such as soil C ($\varepsilon_r = 9$, $\rho = 2000\ \Omega$ m) and soil D ($\varepsilon_r = 36$, $\rho = 2000\ \Omega$ m), the soil permittivity will have some influence on the transient response of the grounding system. Here, the current impulse is still $I(t) = 1 \times (\mathrm{e}^{-14\,300t} - \mathrm{e}^{-5\,400\,000t})$ A. Fig. 9 shows the transient voltages of grid (a) at the injection point A in the soil C and D. The mutual capacitive coupling between the conductors is considered. The peak value of the transient voltages at point A in the soil C is about 6% larger than that in the soil D. On the other hand, the rise time of the transient voltages at point A increases about 3 μs when the grounding system is buried in soil D, compared with that in soil C. This is because the capacitance can delay the phase of the signal and the capacitive coupling is more effective in the soil with very high resitivity. In the soil with lower resistivity, the conduction current is dominant, so, the influence of the soil permittivity on the transient behavior of the grounding system is very small and could be neglected, compared with the influence of the soil resistivity. But, in the soil with extremely high resistivity, the displacement current is not negligible. Comparing Figs. 8 and 9, it is found that the peak values of the transient voltages at point A in soil C and D are increased by about four times compared with that in soil A and B, respectively. This result means that the influence of the soil resistivity is more important than that of the soil permittivity. However, the result of Fig. 9 implies that the influence of the soil permittivity on the transient behavior of the grounding system in the soil with very high resistivity may be considered for better accuracy of results.

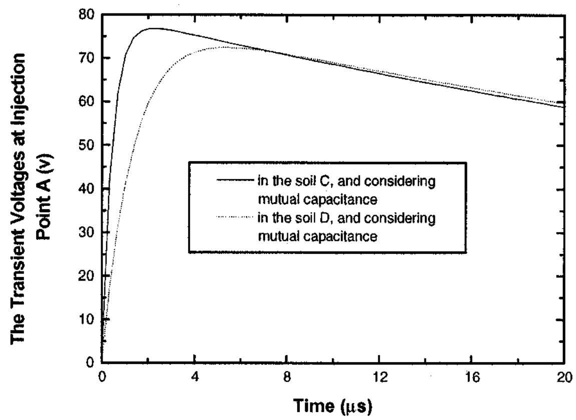

Fig. 9. The transient voltages of grid (a) at point A and B considering the influence of mutual capacitances in diffreent soils C ($\varepsilon_r = 9$, $\rho = 2000\ \Omega$m) and D ($\varepsilon_r = 36$, $\rho = 2000\ \Omega$m).

C. The Influence of the Conductor's Condutivity and Skin Effect

The conductivity and the skin effect of the conductor mainly influence the per-unit length resistance of the conductor. When the radius of the conductor is constant, the per-unit length resistance of the conductor is proportional to the inverse of the conductivity, $r_{\mathrm{dc}} \propto 1/\sigma$. If the injection current impulse includes the high frequency components and the skin depth of the conductor is smaller than the radius of the conductor, the skin effect should be considered. Then, the per-unit length resistance of the conductor will be proportional to the root of the frequency, $r_{HF} \propto \sqrt{f} r_{\mathrm{dc}}$. For example, if one of the frequency components of the lightning current impulse is about 100 kHz,

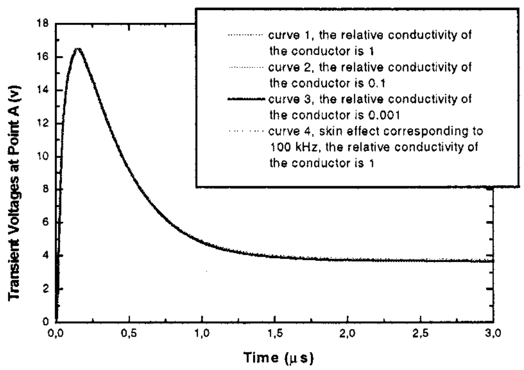

Fig. 10. The transient voltages of the grid (a) at injection point to the remote ground when the influence of the skin effect and the conductivity of the conductor are considered.

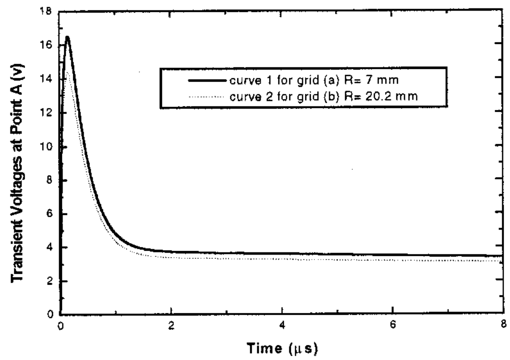

Fig. 11. The transient voltages at the injection point as response to the current impulse with different grid dimensions.

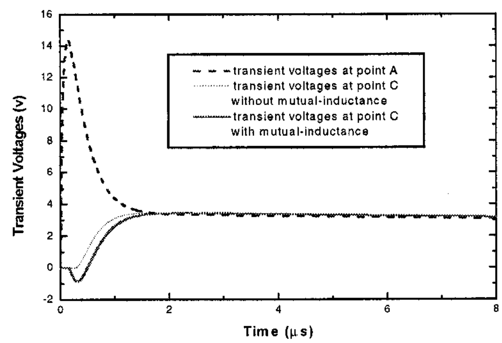

Fig. 12. The influence of the mutual inductance of the grounding system on the transient voltage to the remote ground of grid (b) at point C as response to the current impulse.

for grounding grid (a) (see Fig. 5), the per-unit length resistance of the conductor will be 300 times the dc resistance at this frequency.

Grounding grid (a) (see Fig. 5) is buried at 0.6-m depth in a homogenuous soil with $\rho = 100\Omega\cdot$m and $\varepsilon_r = 36$. The injection current impulse is $I(t) = 1 \times (\mathrm{e}^{-14\,300t} - \mathrm{e}^{-5\,400\,000t})$ A. Fig. 10 shows the transient behavior of grid (a) at injection point A, when the skin effect and different relative conductivities of the conductor are considered. Relative conductivity is defined as the ratio of the conductivity of the material of the wire to that of copper. Curve 1 to 3 are the results for different relative conductivities (1, 0.01 and 0.001). Curve 4 is the result of the influence of the skin effect corresponding to a frequency of 100 kHz. These four curves are almost the same. It means that the influence of the increased resistance of the conductor on the transient behavior of the grounding system is very small, so that the skin effect and resistance of the conductor can be neglected in our model.

D. The Influence of the Grounding Conductors' Diameter

The influence of the grounding conductors' diameter on the transient behavior of the grounding system is more complex than the influence of the soil resistivity and permittivity, because when the diameter of the conductor changes, the per-unit length resistance and inductance of the conductor will be different. Also the conductance and the capacitance will change with the changing of the conductor diameter.

Grounding grid (a) and (b) (see Fig. 5) are buried at 0.6-m depth in a homogenuous soil with $\rho = 100\ \Omega$m and $\varepsilon_r = 36$. When the radius of the conductor increases from 7 to 20.2 mm, the per-unit length parameters of the grounding conductors will be changed. The self inductance decreases about 13%, and the resistance of the conductor decreases almost 10 times, while the capacitance increases about 8% and the conductance of conductor to the ground increase about 10%. Here, the change of the capacitance is neglected because its influence is very small as seen in the earlier section. Fig. 11 presents the transient voltages to the remote ground at the injection point of these two different grids as response to the current impulse $I(t) = 1 \times (\mathrm{e}^{-14\,300t} - \mathrm{e}^{-5\,400\,000t})$ A. Curve 1 is for grid (a), and curve 2 shows the result of grid (b). It is clear that increasing the diameter of the conductor can decrease the transient voltage at the injection point. Here, the influence of the decrease in resistance on the transient behavior of the grounding system could be the smallest, because the resistance of the conductor is much smaller than the impedance of the self inductance when the current changes very fast, and also much smaller than the resistance of the conductor to the ground. Consequently, increasing the diameter of the conductor is advantageous to decrease the peak value of the transient voltage of the grounding system at injection point mainly because of the decrease of the self inductance and the increase of the conductance of the conductor to the ground. This result indirectly shows that the soil ionization can help the grounding system to dissipate the current and decrease the transient voltage faster [11], because according to the generally accepted model of the transient behavior of the grounding rod in [14], that considered the soil ionization, the soil ionization is assumed to be homogeneous and represented by the increase of the dimension of the conductor.

Fig. 12 compares the transient voltages to the remote ground of grid (b) (see Fig. 5) at point C, with and without considering the mutual inductance between the conductors. When the mutual inductance is included, there is a negative going part during the first several hundred ns. This behavior is perhaps due to the mutual inductive coupling between the conductors. It can be explained as follows. The mutual inductive coupling between the conductors will introduce a voltage source, $V = -M(dI/dt)$, from one current loop of the grid to another current loop. At the beginning of the lightning-current impulse, $dI/dt \gg 0$, so that the induced voltage will be very large and could be opposite to the ordinary voltage drop between two points in the loop. This may cause a negative voltage at the beginning of the current impulse as shown in Fig. 12 at point C and in Fig. 7 at points F, E, and C.

V. Conclusion

An improved transmission line model of the grounding system is presented.

- It is a time-domain model of the grounding system, which can be more easily used in EMC and lightning-protection studies, especially when the grounding system is combined with other nonlinear protection components, such as varistor and gas discharge tube.
- Mutual electromagnetic coupling between the different parts of the grounding structure and the influence of air-earth interface are considered. The model is implemented in ATP-EMTP.

Simulation results of this model fit to the results of the complex model based on full solution of the Maxwell's equations [1], [2] very well. The influence of different parameters of the grounding system are analyzed and explained from the point of electric circuit theory. It shows that the influence of the soil resistivity is much larger than that of any other parameters for bare buried conductor system. Higher soil resistivity introduces more serious voltage difference at different parts of the grounding system, especially at the beginning of the current impulse. A four-time increase in the soil resistivity produces a four-time increase in the equalized voltage on the surface of the grounding system. The influence of conductivity and the skin effect of the conductor can be neglected. Variation of the soil permittivity, keeping soil conductivity a constant, does not have much influence on the transient response of the grounding system except in soils with extremely high resistivity. Increasing the diameter of the conductor tends to reduce the transient voltage of the grounding system.

Acknowledgment

The authors wish to thank V. Scuka for many helpful comments that enabled to improve the paper, and Adtranz Signal AB (contact person H. Lind), for funding this research.

References

[1] L. D. Grcev, "Computer analysis of transient voltages in large grounding systems," *1995 IEEE Trans. Power Delivery*, vol. 11, pp. 815–823, Apr. 1996.

[2] L. D. Grcev and M. Heimbach, "Frequency dependent and transient characteristics of substation grounding system," *IEEE Trans. Power Delivery*, vol. 12, pp. 172–178, Jan. 1997.

[3] B. G. Gupta and B. Thapar, "Impulse impedance of grounding grids," *IEEE Trans. Power App. Syst.*, vol. PAS-99, pp. 2357–2362, Nov./Dec. 1980.

[4] M. Ramamoorty, M. M. B. Narayanan, and S. Parameswaran *et al.*, "Transient performance of grounding grids," *IEEE Trans. Power Delivery*, vol. 4, pp. 2053–2059, Oct. 1989.

[5] A. P. Meliopulos and M. G. Moharam, "Transient analysis of grounding systems," *IEEE Trans. Power App. Syst.*, vol. PAS-102, pp. 389–399, Feb. 1983.

[6] A. D. Papalexopoulos and A. P. Meliopulos, "Frequency dependent characteristics of grounding systems," *IEEE Trans. Power Delivery*, vol. 2, pp. 1073–1081, Oct. 1987.

[7] M. Heimbach and L. D. Grcev, "Grounding system analysis in transients programs applying electromegnetic field approach," *IEEE Trans. Power Delivery*, vol. 12, pp. 186–193, Jan. 1997.

[8] L. Grcev and F. Dawalibi, "An electromagnetic model for transients in grounding system," *IEEE Trans. Power Delivery*, vol. 5, pp. 1773–1781, Nov. 1990.

[9] *Ace version 2.51, ABB common platform for 2D field analysis and simulation*, ABB Corporate Research, Västerås, Sweden, 1998.

[10] *ATP rule book*, Can/Am EMTP User Group, 1995.

[11] A. Geri, "Behavior of grounding systems excited by high impulse currents: the model and its validation," *IEEE Trans. Power Delivery*, vol. 14, pp. 1008–1017, July 1999.

[12] C. Nordling and J. Östetman, *Physics Handbook for Science and Engineering*. Lund, Sweden: Studentlitteratur, p. 213.

[13] C. R. Paul, *Introduction to Electromagnetic Compatibility*. New York: Wiley, p. 127.

[14] A. C. Liew and M. Darveniza, "Dynamic model of impulse characteristics of concentrated earth," *Proc. Inst. Elect. Eng.*, vol. 121, pp. 123–135, Feb. 1974.

[15] W. Blumer and M. Ianovici, "Calculation of the propagation constant of buried insulated conductors," in *Proc. 5th Int. Symp. Electromagnetic Compatibility*, Zurich, Germany, Mar. 10–12, 1983, Paper 10C3.

[16] J. H. Head, "Propagation constants of an insulated conductor buried in a stratified medium. The air–earth and soil-rock interfaces,", Note 52, AFWL-EMP 3-4, 1970.

Yaqing Liu was born in Jiangsu, China, in 1969. She received the M.S. degree in plasma physics, from the Shanghai Institute of Optics and Fine Machine, Academy of Chinese Science, Shanghai, China, in 1996. She is working toward the Ph.D. degree at the Division for Electricity and Lightning Research, Ångström Laboratory, Uppsala University, Uppsala, Sweden.

Her research area is electromagnatic compatibility.

Mihael Zitnik received the Bachelor's degree in electrical engineering degree from the University of Maribor, Maribor, Slovenija, and the Licentiate of Technology degree from Uppsala University, Uppsala, Sweden, in 1996, and 1999, respectively. He is currently working toward the doctoral degree at the Uppsala University.

His research is in the area of high-voltage engineering, lightning protection, and EMC.

Rajeev Thottappillil was born in Kerala, India in 1958. He received the B.Sc. degree in electrical engineering from the University of Calicut, Calicut, India, in 1981, and the M.S. and Ph.D. degrees in electrical engineering from the University of Florida, Gainesville, in 1989, and 1992, respectively.

Since 1995, he is with the Uppsala University, Uppsala, Sweden where he is currently a Professor in the division for electricity and lightning research. His main research interests are electromagnetic compatibility, lightning, and electromagnetic theory.